

The Effect of Alloying Elements on the Metastable Zr Solid Solubility and Precipitation of $L1_2$ Al_3Zr Precipitates in Aluminium Alloys

Zhihong Jia¹, Jesper Friis^{1,2}, Børge Forbord^{2,3}, Jan Ketil Solberg¹, and Knut Marthinsen²

¹Department of Materials Science and Engineering, Norwegian University of Science and Technology (NTNU), N-7491 Trondheim, Norway

²SINTEF Materials and Chemistry, N-7465 Trondheim, Norway

³Scandpower AS, N-7462 Trondheim, Norway

Metastable $L1_2$ Al_3Zr precipitates have been found to be very efficient in resisting the recrystallisation of aluminium alloys. Precipitation of Al_3Zr precipitates can be modified by other existent alloying elements in multi-component aluminium alloys through various mechanisms. One of them is that addition of alloying elements could change Zr solubility and thus, result in variation of amount of Al_3Zr precipitates. In this work, three alloying elements, Mn, Si, Fe, often used or found in aluminium alloys and their effects on Zr solubility and $L1_2$ Al_3Zr precipitation have been investigated. A model for calculating zirconium solid solubility has been developed and compared with Thermo-Calc calculations. The present model is based on the CALPHAD method using the COST507 database and is suitable for estimations of metastable zirconium solubility. Application of the model to an Al-Zr alloy containing Mn, Si and/or Fe predicts that Si decreases and Mn increases the metastable zirconium solubility, whereas Fe appears to have no influence. Experimental investigations by TEM are in agreement with the model prediction.

Keywords: Aluminium alloy, Zirconium, Precipitation, Modelling, Transmission Electron Microscopy

1. Introduction

Additions of zirconium and subsequent formation of Al_3Zr -precipitation hinder recrystallisation of aluminium alloys during thermomechanical processing by exerting a drag force (Zener-drag) on moving subgrain-/grain boundaries. Al_3Zr can crystallize in the stable tetragonal DO_{23} or the metastable cubic $L1_2$ crystal structure [1]. The latter crystal structure is coherent with the aluminium matrix and very efficiently promotes a high recrystallization resistance through the formation of a high density of small precipitates.

Other alloying elements like lithium, magnesium, copper, zinc etc. may, however, significantly affect the precipitation kinetics of Al_3Zr by altering the level and distribution of Al_3Zr precipitates compared to that of a binary Al-Zr alloy [2-6]. Calculations of phase equilibrium in Al-Li-Zr alloys have for instance shown that the solubility of zirconium is drastically reduced when lithium is present [7]. Sigli [8] has proposed a model for the interactions between elements in solid solution. The metastable zirconium solubility was evaluated by neglecting the influence of other possible phases in multi-elements alloys, and the efficiency of the alloying elements in decreasing the zirconium solubility was found to be in the order $Zn < Cu < Mg < Li$. The effect on Al_3Zr precipitation of adding other alloying elements, like Si, Fe, Mn and Sc, to Zr-containing aluminium alloys has also been studied experimentally [5, 9-10], and these elements have been found to enhance Al_3Zr -precipitation. Especially distinct improvements of the number density and distribution of Al_3Zr precipitates have been observed by TEM when scandium is added.

Westengen et al. [5] have discussed possible reasons for the positive effects of Si and Fe. The elements may act as nucleation sites lowering the Al_3Zr nucleation barrier, and/or be incorporated in the nucleus, which lowers the interface boundary energy or the volume free energy of the precipitates. Forbord et al. [9] proposed another possible explanation, that additions of Mn, Si and Fe may decrease the solid solubility of zirconium in aluminium and thus increase the driving force for

forming Al₃Zr precipitates. In conclusion, the nature of the stimulating effect of these elements on Al₃Zr precipitation is not yet really clear. In the present work, we have calculated the metastable zirconium solubility in Al-Zr alloys, with and without additions of Mn, Si and/or Fe in order to better understand the effect of these elements. Scandium is, however, not included in the calculations because Zr atoms segregate to Sc-rich clusters and form Al₃(Sc,Zr)-precipitates [11], and this behaviour do not fit into the present model.

2. The model and experimental methods

2.1 The model

The alloying system is modelled as a solid solution (α -Al phase) in thermodynamical equilibrium with Al₃Zr precipitates (named as the P-phase). The molar Gibbs free energy of the solid solution is written as

$$G^\alpha = \sum_i x_i^\alpha G_i^0 + RT \sum_i x_i^\alpha \ln(x_i^\alpha) + G^{\alpha, xs}, \quad (1)$$

where x_i^α is the mole fraction of element i in solid solution, G_i^0 is the Gibbs free energy for the pure element i , $G_i^{\alpha, xs}$ is the excess Gibbs energy, and R and T are the gas constant and temperature, respectively. Only binary interactions are included in the excess energy, which is expressed in terms of Redlich-Kister polynomials as

$$G^{\alpha, xs} = \sum_i \sum_{j>i} x_i^\alpha x_j^\alpha \sum_{v \geq 0} L_{ij}^{v, \alpha} (x_i^\alpha - x_j^\alpha)^v, \quad (2)$$

where L_{ij}^v are (temperature dependent) Redlich-Kister coefficients, obtained from the COST 507 database [12]. The chemical potentials for the solid solution are calculated as

$$\mu_i^\alpha = \frac{\partial G^\alpha}{\partial x_i^\alpha} + G^\alpha - \sum_j x_j^\alpha \frac{\partial G^\alpha}{\partial x_j^\alpha} = G_i^0 + RT \ln(x_i^\alpha) + \mu_i^{\alpha, xs}, \quad (3)$$

where

$$\mu_i^{\alpha, xs} = \sum_{j \neq i} \sum_v Q_{ij}^v x_j^\alpha \left[(x_i^\alpha - x_j^\alpha)^v + v x_i^\alpha (x_i^\alpha - x_j^\alpha)^{v-1} \right] - \sum_j \sum_{k>j} x_j^\alpha x_k^\alpha \sum_v Q_{jk}^v (v+1) (x_j^\alpha - x_k^\alpha)^v, \quad (4)$$

is the excess energy contribution, and Q_{ij}^v are *modified Redlich-Kister coefficients*, defined as

$$Q_{ij}^v = \begin{cases} L_{ij}^v, & i < j \\ 0, & i = j \\ (-1)^v L_{ij}^v, & i > j \end{cases} \quad (5)$$

The molar Gibbs free energy of Al₃Zr with L1₂ structure is given by

$$G^P = 3\mu_{Al}^P + \mu_{Zr}^P = 3\mu_{Al}^\alpha + \mu_{Zr}^\alpha, \quad (6)$$

where the last relation follows from the assumption of thermodynamical equilibrium. The formation enthalpy $\Delta H^P = -162.5$ kJ/mol and entropy $\Delta S^P = -28.9$ J/(mol·K) for Al₃Zr are obtained from the FTLite FactSage database [12]. We can also write the Gibbs free energy for Al₃Zr as

$$G^P = 3G_{Al}^0 + G_{Zr}^0 + \Delta H^P - T\Delta S^P. \quad (7)$$

Combining Eq. (3) with Eqs. (6-7) leads to the solubility product

$$\prod_i (x_i^\alpha)^{n_i^p} = \exp\left(\frac{\Delta H - T\Delta S - \sum_i n_i^p \mu_i^{\alpha, \text{xs}}}{RT}\right). \quad (8)$$

In order to solve Eq. (8) with respect to x_{Zr} , we need to express x_i in terms of x_{Zr} for $i \neq \text{Zr}$. This is done by considering the nominal content of element i

$$x_i^0 = f x_i^p + (1-f)x_i^\alpha, \quad (9)$$

where f is the mole fraction of Al_3Zr . Hence, the mole fraction of element i in solid solution is

$$x_i^\alpha = \frac{x_i^0 - f x_i^p}{1-f}, \quad \text{with } f = \frac{x_{\text{Zr}}^0 - x_{\text{Zr}}^\alpha}{x_{\text{Zr}}^p - x_{\text{Zr}}^\alpha}. \quad (10)$$

The formalism presented here is an extension of the regular solution model, consistent with the CALPHAD method. Even though all this can be accomplished with fewer approximations in commercial software like Thermo-Calc and FactSage, not everyone has access to these. Therefore simple models, like the above formalism have a value by its own.

Five experimental alloys [3, 9, 14-15], for which the chemical compositions are listed in Table 1, have been considered. Calculations of the metastable zirconium solubility have been performed by using the present model. Only the α matrix phase and Al_3Zr were considered and only binary interactions between elements were included.

Table 1 Chemical composition of the alloys, in wt%

No.	Alloy	Zr	Mn	Si	Fe
1	AlZr (HP)	0.15			
2	AlZrMn (HP)	0.15	1.01		
3	AlZrSi (HP)	0.15		0.14	
4	AlZrSiFe (CP)	0.18		0.16	0.20
5	AlZrMnSiFe (CP)	0.15	1.01	0.15	0.21

HP - high purity, CP - commercial purity.

2.2 Experimental procedures

The alloys (Al-0.15 wt.%Zr and Al-0.15 wt.%Zr-1.0 wt.%Mn) investigated in this work were direct chill cast at a temperature of $\sim 700^\circ\text{C}$ and subsequently water-quenched. The billet has column shape with diameter 100 mm and height 180 mm. The samples cut from the bulk material were homogenized at 630°C for 240 h and/or precipitation annealed at 450°C for 100 h in an air-circulating furnace, followed by immediate water-quenching.

A JEOL 2010 transmission electron microscopy (TEM) operated at 200 keV was used for investigations of precipitates. An electron energy loss spectrometer was applied for measuring thickness of the samples where the images were taken, in order to calculate the volume fraction of precipitates. The TEM samples were prepared by electro-thinning in 75% methanol and 25% nitric acid in a Struers Tenupol at a temperature of -30°C .

3. Results and discussion

Figure 1 shows the zirconium solubility in the binary Al-Zr alloy as calculated by both the present model and by Thermo-Calc. Two databases, COST507 and TTAL3 have been used in the Thermo-Calc calculation, and only COST507 in the calculation based on the present model. (TTAL is produced by N. Saunders, and the authors have used it with permission from Hydro Aluminium.) The two methods give quite different values for the zirconium solubility in aluminium solid solution. The reason is analysed as follows: the present model explicitly defines the unit cell of the precipitates to

contain 3 Al and 1 Zr atom, so the calculation gives the solubility in equilibrium with the metastable $L1_2$ phase, which is in good agreement with that from first-principle calculations [1]. The Thermo-Calc calculations using the COST507 database, however, include the small displacements that make the unit cell 4 times larger and give the solubility in equilibrium with the stable DO_{23} phase [16]. In addition, the Thermo-Calc calculations using the TTAL3 database give an abnormal right shift of the solubility curve which implies higher solubility. FactSage calculations using either of the databases give similar results as Thermo-Calc. The reason why the TTAL3 database gives this odd result is not yet clear.

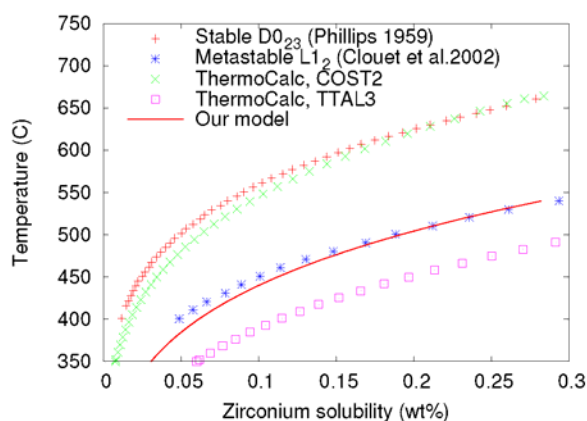


Fig. 1 Zirconium solubility in the binary Al-Zr alloy calculated by both the present model and the Thermo-Calc method using COST 507 and TTAL3 databases. Literature data for Zr solubility in the presence of stable DO_{23} and metastable $L1_2$ are given for comparison.

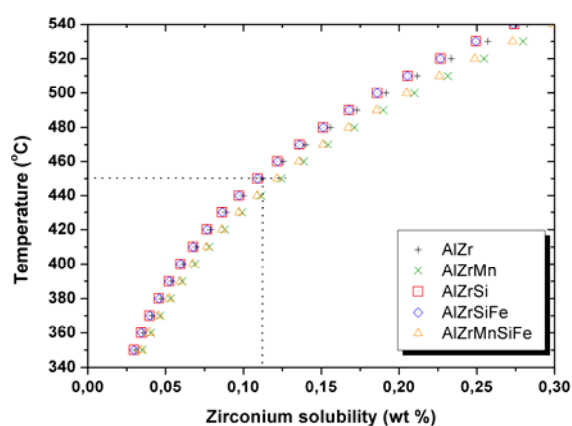


Fig. 2 Zirconium solubility curves in equilibrium with metastable Al_3Zr precipitates in five alloys, calculated by the present model. The zirconium solubility at $450^\circ C$ is indicated by the dotted line.

In the present work, we mainly focus on the Zr solubility in equilibrium with the metastable $L1_2$ phase. From the above comparison, the present model gives a reasonable prediction of the metastable solubility of zirconium. Therefore, the model has been applied to ternary alloy systems to study the effect of alloying elements on the solubility of zirconium in equilibrium with metastable zirconium precipitates. Figure 2 shows the zirconium solvus in equilibrium with metastable Al_3Zr for five selected alloys calculated by the model. Additions of alloying elements give small changes of the Zr solubility. In the present simplified model it is assumed that the alloying elements are present in solid solution, although some multi-component phases have been observed in very low amounts. The addition of Mn leads to an increase in the zirconium solubility, whereas Si-additions lead to a slight decrease in the zirconium solubility. An almost complete overlap between the Zr solvus of the ternary $AlZrSi$ alloy and the quaternary $AlZrSiFe$ alloy indicates that the effect of Fe-additions on the zirconium solubility is negligible. The zirconium solubility at $450^\circ C$ is about 0.11 wt% according to the present model (Figure 2) and about 0.19 wt% using Thermo-Calc and the TTAL3 database (Figure 1). Since the concentration of zirconium in the binary Al-Zr alloy is 0.15 wt%, there should be metastable Al_3Zr precipitates in the alloy after annealing at $450^\circ C$ according to the present model. This result is, however, not in agreement with the Thermo-Calc calculation.

TEM investigations of the high-purity Al-0.15 wt% Zr alloy, homogenized at $630^\circ C$ for 240 h and precipitation annealed at $450^\circ C$ for 100 h, have been carried out. The purpose of the homogenization treatment of the alloy before the precipitation annealing is to eliminate the zirconium segregation from the casting, which may lead to an early precipitation in zirconium-enriched regions. The results of the homogenization treatment showed that the zirconium segregation was greatly removed [14]. Figure 3a is a diffraction pattern from the Al-Zr alloy sample, for which the projection direction is some degrees off $[100]$ in order to obtain higher intensities in some of the superreflections. The

superreflections located midway between 000 and 022, or equivalent pairs of reflections, indicate that there is a coherent relationship between the metastable $L1_2$ phase of the Al_3Zr precipitates and the Al matrix. By selecting the superreflection that is marked in Figure 3a, the TEM dark field image of Figure 3b was obtained. A dense distribution of metastable Al_3Zr precipitates with a diameter in the range of 30-50 nm was observed. This observation supports the present model prediction that zirconium is in a supersaturated condition at 450°C, and indicates that the Thermo-Calc calculation based on the TTAL database overestimates the metastable zirconium solubility.

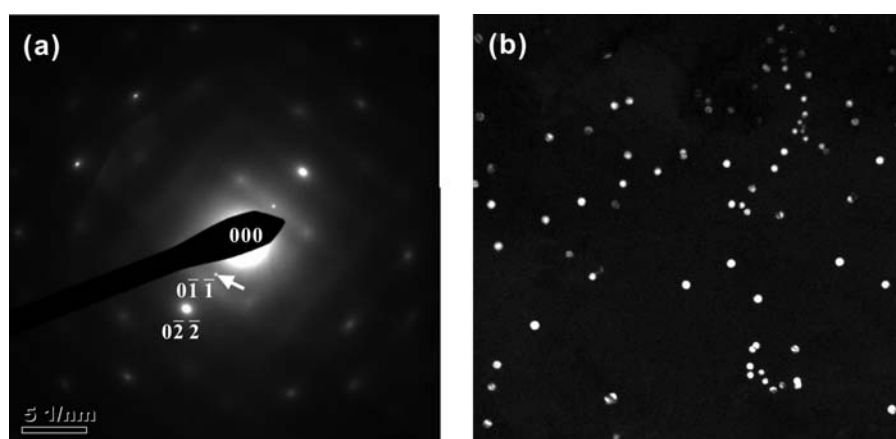


Fig. 3 (a) Diffraction pattern from the Al-0.15 wt% Zr alloy showing the main diffraction- and superreflections. (b) TEM dark field image using the diffraction spot indicated by the arrow in (a) shows metastable Al_3Zr precipitates. The specimen was homogenized at 630°C for 240 h followed by water quenching, and subsequently precipitation annealed at 450°C for 100 h.

As far as the Mn-addition is concerned, a negative effect on Al_3Zr precipitation is predicted by the present model, while experimental work by some of the present authors [9] indicates that the effect should be positive. In order to clarify this inconsistency, TEM investigations of a high purity binary Al-Zr alloy and a high purity ternary Al-Zr-Mn alloy, only annealed at 450°C for 100h, were carried out, Figure 4. It is evident from the results that there are more Al_3Zr precipitates in the binary alloy than in the ternary alloy. The volume fraction of Al_3Zr precipitates averaged from ten randomly taken images was 1.9×10^{-3} for the Al-Zr alloy and 1.2×10^{-3} for the Al-Zr-Mn alloy.

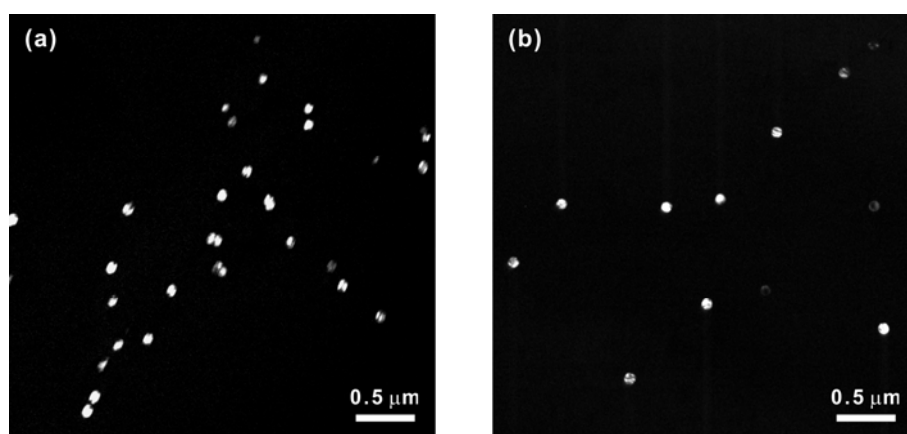


Fig. 4 TEM dark field images from (a) Al-Zr alloy and (b) Al-Zr-Mn alloy. Both alloys were precipitation annealed at 450°C for 100 h.

The experimental result in ref. [9] is therefore assumed to be due to the combined presence of Si and Mn (and possibly also Fe) and not from Mn alone. This assumption is supported by both experiments and the present model [5, 9] which indicate that Si-additions promote the formation of Al_3Zr precipitates. A large number of Al_3Zr precipitates were observed in the Al-Zr-Si alloy annealed at 450°C for 12h, but no Al_3Zr precipitates were observed in the binary Al-Zr alloy in the same condition. Previously, it has been assumed that Si-atom clusters may act as nucleation sites and lower the nucleation barrier for the Al_3Zr phase, an explanation that is supported by the fact that Al_3Zr precipitates nucleate both from homogeneous and heterogeneous sites in the Al-Si-Zr alloy [3]. The

present calculations predict that the effect of Si-additions on the precipitation of Al₃Zr precipitates can also be due to decreased zirconium solubility in aluminium solid solution.

As judged from Figure 2, Fe-additions are not expected to have any influence on the Zr solubility in aluminium, and thus, on the volume fraction of Al₃Zr precipitates. However, a distinct increase in the number density and volume fraction of Al₃Zr precipitates is found upon adding Fe [9]. This observation could be due to a similar mechanism as for Si, i.e. that Fe atoms promote Al₃Zr nucleation by forming clusters acting as nucleation sites by lowering the Al₃Zr nucleation barrier. Moreover, Fe seems to be more efficient than Si in this respect.

4. Conclusions

The model presented in this work is suitable for calculating the metastable L1₂ zirconium solubility. Thermo-Calc using the COST507 database gives the zirconium solubility in equilibrium with stable DO₂₃. The model has been applied on five selected aluminium alloys and reveals different influences of Si, Fe and Mn on the metastable Zr solubility. Si and Mn decreases and increases the zirconium solubility, respectively, whereas Fe appears to have no influence on the solubility. The large number of Al₃Zr precipitates observed in Si-containing Al-Zr alloys may be attributed to both the increase of the driving force for Al₃Zr nucleation and the lowering of the Al₃Zr nucleation barrier by Si-atom clusters acting as nucleating sites. Fe does not lower the Zr-solubility, but is even more effective than Si in enhancing the nucleation rate of the Al₃Zr precipitates. Mn, however, weakens the precipitation capability of Al₃Zr precipitates by increasing the solid solubility of zirconium in aluminium.

The authors would like to thank Dr. Kai Tang (SINTEF, Materials and Chemistry) for the FactSage calculation. Financial support from the Norwegian Research Council is gratefully acknowledged.

References

- [1] E. Clouet, J.M. Sanchez, C. Sigli, *Physical Review B*, 65 (2002) 094105.
- [2] M. Kanno, B.L. Ou, *Scripta Metall.*, 24 (1990) 1995-2000.
- [3] K. Ranganathan, H.R. Last, T.H. Sanders, in: L. Arnberg, O. Lohne, E. Nes, N. Ryum (Eds.) *The 3rd International Conference on Aluminium Alloys*, Trondheim, Norway, 1992, pp. 15-20.
- [4] D. Srinivasan, K. Chattopadhyay, *Metallurgical and Materials Transactions*, 36A (2005) 311-320.
- [5] H. Westengen, O. Reiso, L. Auran, *Aluminium*, 12 (1980) 768-775.
- [6] J.D. Robson, P.B. Prangnell, *Materials Science and Engineering*, 352A (2003) 240-250.
- [7] N. Saunders, *Zeitschrift Fur Metallkunde*, 80 (1989) 894-903.
- [8] C. Sigli, in: J.F. Nie, A.J. Morton, B.C. Muddle (Eds.) *The 9th International Conference on Aluminium Alloys* (Institute of Materials Engineering Australasia Ltd, Brisbane, Australia, 2004, pp. 1353-1358.
- [9] B. Forbord, H. Hallem, K. Marthinsen, in: J. Nie, A. Morton, B. Muddle (Eds.) *Materials Forum*, Institute of Materials Engineering Australasia Ltd, Brisbane, Australia, 2004, pp. 1179-1185.
- [10] Y.W. Riddle, H. Hallem, N. Ryum, *Mater Sci Forum*, 396-402 (2002) 563-568.
- [11] B. Forbord, W. Lefebvre, F. Danoix, H. Hallem, K. Marthinsen, *Scripta mater.*, 51 (2004) 333-337.
- [12] [FTlite database, 2009, www.factsage.com].
- [13] I. Ansara, A.T. Dinsdale, M.H. Rand, in: *Cost 507*, European Commission, 1998.
- [14] B. Forbord, H. Hallem, K. Marthinsen, in: J. Nie, A. Morton, B. Muddle (Eds.) *Materials Forum*, (Institute of Materials Engineering Australasia Ltd, Brisbane, Australia, 2004), pp. 1263-1269.
- [15] Z.H. Jia, G.Q. Hu, B. Forbord, J.K. Solberg, *Materials Science and Engineering*, 444A (2007) 284-290.
- [16] H.W.L. Phillipps, *Annotated equilibrium diagrams of some aluminium alloy systems* (Institute of Metals, 1959).